Solid State Communications 366-367 (2023) 115154

Contents lists available at ScienceDirect

Solid State Communications

journal homepage: www.elsevier.com/locate/ssc

Strain-gradient-modulated Kondo effect at the $LaAlO_3$/$SrTiO_3$ heterointerface

Weimin Jiang [a,b,1], Qiang Zhao [b,1], Zhe Zhang [b], Tingna Shao [b], Zitao Zhang [b], Mingrui Liu [c], Chunli Yao [b], Yujie Qiao [b], Meihui Chen [b], Xingyu Chen [b], Ruifen Dou [b,***], Changmin Xiong [b,**], Jiacai Nie [b,*]

[a] School of Science, Heilongjiang University of Science and Technology, Harbin 150022, People's Republic of China
[b] Department of Physics, Beijing Normal University, Beijing 100875, People's Republic of China
[c] State Key Laboratory of Luminescence and Applications, Changchun Institute of Optics, Fine Mechanics and Physics, Chinese Academy of Sciences, Changchun, 130033, People's Republic of China

ARTICLE INFO

Communicated by: E.Y. Andrei

Keywords:
Strain gradient
Kondo effect
$LaAlO_3$/$SrTiO_3$
2DEG

ABSTRACT

Modulation of Kondo phenomenon in two-dimensional materials is of great significance. Unfortunately, the strain effect, one of the effective regulation methods, is usually lacking in previously studied Kondo systems. Here we show that a tensile or compressive strain gradient induced by a three-point bending apparatus has a prominent impact on Kondo effect of the two dimensional electron gas at the $LaAlO_3$/$SrTiO_3$ heterointerface. Under the tensile strain gradient, Kondo temperature (T_K) decreases. In contrast, T_K increases under the compressive strain gradient. At the same time, the temperature at which the resistance has a minimum, T_{min}, shows the same strain gradient dependence as T_K. The present study may pave the way for manipulating many-body effects at oxide heterointerface.

1. Introduction

The Kondo effect, the screening of the local magnetic moment by itinerant electrons, is a many-body quantum phenomenon which usually leads to a pronounced Kondo scattering at low temperatures [1]. The development of low dimensional systems offers a new opportunity to exploit the emergent aspects of the Kondo effect [2,3]. Recently, $LaAlO_3$/$SrTiO_3$ (LAO/STO) interface with high mobility two dimensional electron gas (2DEG) has aroused much attention [4,5]. A spectrum of emergent properties has been unveiled in this system, including Rashba spin-orbit coupling [6,7] and superconductivity [8] and the coexistence of magnetism and superconductivity [9,10]. In particular, this oxide interface can form a natural all-*d*-electron 2D Kondo system. The Kondo effect in this 2DEG has already been deduced from the resistance upturn with decreasing temperature [11,12] and the Kondo resonance in the planar tunneling junctions [11]. The large negative magnetoresistance observed in this 2DEG has also been attributed to the Kondo effect [13].

On the other hand, modulating the LAO/STO properties is an important research issue. So far, the means of modulation reported at the LAO/STO interface contain gate voltage [14] light irradiation [15] and surface adsorption [16] etc. An epitaxial strain produced by the lattice mismatch between different films and substrates can also affect the electrical properties at the LAO/STO heterointerface [17–21] and other STO-based heterointerface [22]. However, the impact of epitaxial strain is always biaxial and static, ignoring the study of the strain impact in a dynamic process. Recently, Zhang Z. et al. Revealed the strain-gradient-induced modulation of carrier density and mobility at the LAO/STO interface by a mechanical bending [23]. Zhang F. et al. Also demonstrated that dynamic modulation using uniaxial strain on the interfacial transport properties of the LAO/STO interface is effective [24].

As far as we know, Kondo problems in oxide interface are far from clear up to now and how the strain gradient modulates the Kondo effect has not yet been studied at the LAO/STO heterointerface. In this work,

* Corresponding author.
** Corresponding author.
*** Corresponding author.
E-mail addresses: ruifendou@bnu.edu.cn (R. Dou), cmxiong@bnu.edu.cn (C. Xiong), jcnie@bnu.edu.cn (J. Nie).
[1] These authors contributed equally to this work.

https://doi.org/10.1016/j.ssc.2023.115154
Received 29 May 2022; Received in revised form 7 November 2022; Accepted 28 March 2023
Available online 5 April 2023

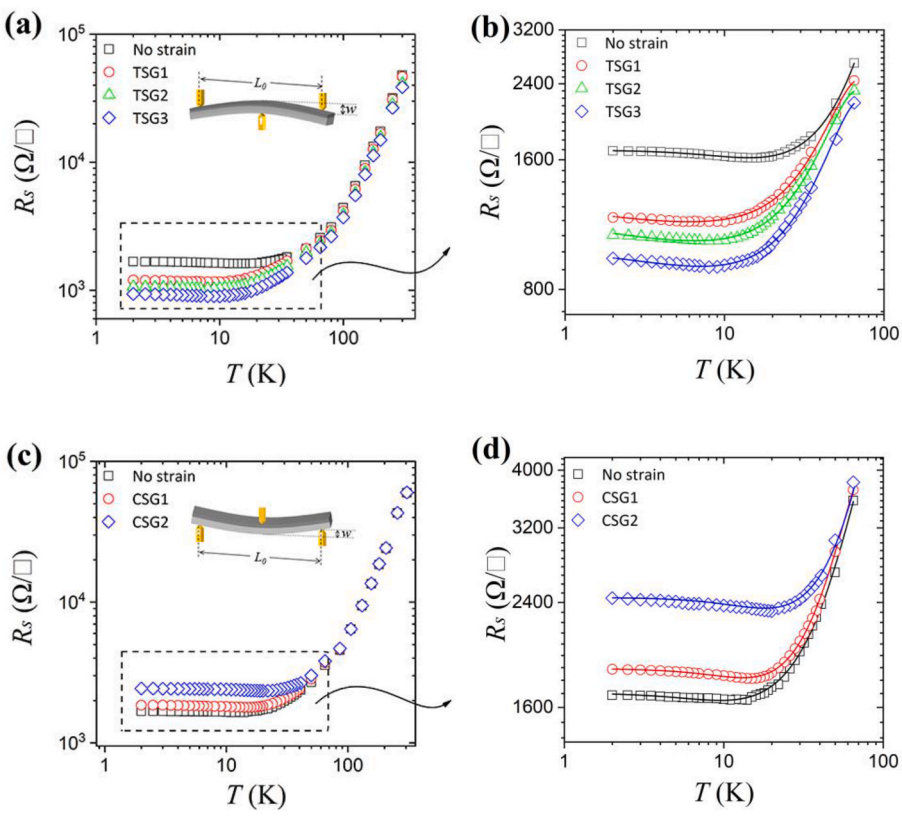

Fig. 1. Temperature-dependent resistance (R_s -T) of two samples. (a) Sample An under TSGs from 2 K to 300 K. (b) Zoom-in on the low-temperature region of (a). (c) Sample B under CSGs from 2 K to 300 K. (d) Zoom-in on the low-temperature region of (c). The solid curves in (b) and (d) show the best fits to R_s-T curves using Eq. (2) and Eq. (3). The inset in (a) and (c) show the schematic structures of tensile and compressive strain bending, respectively. The light and dark grey parts represent STO and LAO, respectively. The white arrows represent the applied strain direction. The yellow parts represent the spring pins which are made of brass. (For interpretation of the references to colour in this figure legend, the reader is referred to the Web version of this article.)

Table 1
Different strain gradients at room temperature.

	CSG2	CSG1	No strain	TSG1	TSG2	TSG3
Strain gradient (m^{-1})	−8.54 ± 0.56	−6.32 ± 0.75	0	+5.85 ± 0.75	+7.93 ± 0.56	+12.24 ± 0.47

Table 2
Fitting parameters extracted from fitting R_s data of LAO/STO heterointerface under different tensile strain gradients.

Strain gradients (m^{-1})	R_0 (Ω/□)	a (Ω/□·K^{-2})	b (Ω/□·K^{-5})	$R_{K,0K}$ (Ω/□)	T_K (K)
0	1454.9	0.18	2.9×10^{-8}	250.5	10.47
+5.85 ± 0.75	1049.6	0.15	2.5×10^{-8}	148.3	7.6
+7.93 ± 0.56	967.7	0.14	2.1×10^{-8}	131.1	5.73
+12.24 ± 0.47	873.2	0.12	1.3×10^{-8}	103.9	5.53

Table 3
Fitting parameters extracted from fitting R_s data of LAO/STO heterointerface under different compressive strain gradients.

Strain gradients (m^{-1})	R_0 (Ω/□)	a (Ω/□·K^{-2})	b (Ω/□·K^{-5})	$R_{K,0K}$ (Ω/□)	T_K (K)
0	1447.4	0.19	3.1×10^{-8}	261.8	9.86
−6.32 ± 0.75	1579.2	0.24	4.9×10^{-8}	310.6	11.15
−8.54 ± 0.56	2058.5	0.29	8.8×10^{-8}	426.1	13.12

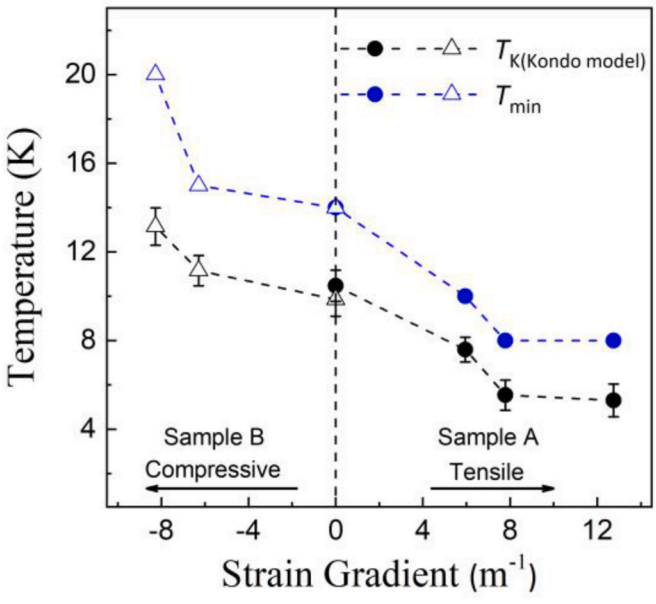

Fig. 2. The relationship between $T_{K(Kondo\ model)}$, T_{min} and uniaxial different strain gradients. The solid circles and hollow triangles represent the $T_{K(Kondo\ model)}$ and T_{min} values under TSGs (sample A) and CSGs (sample B), respectively.

the Kondo effect at the LAO/STO interface modulated by a strain gradient is systematically studied.

2. Experimental section

LAO films with 10 nm were grown on (001)-oriented TiO_2-terminated STO single-crystal substrate (10 × 3 × 0.2 mm^3) by pulsed laser

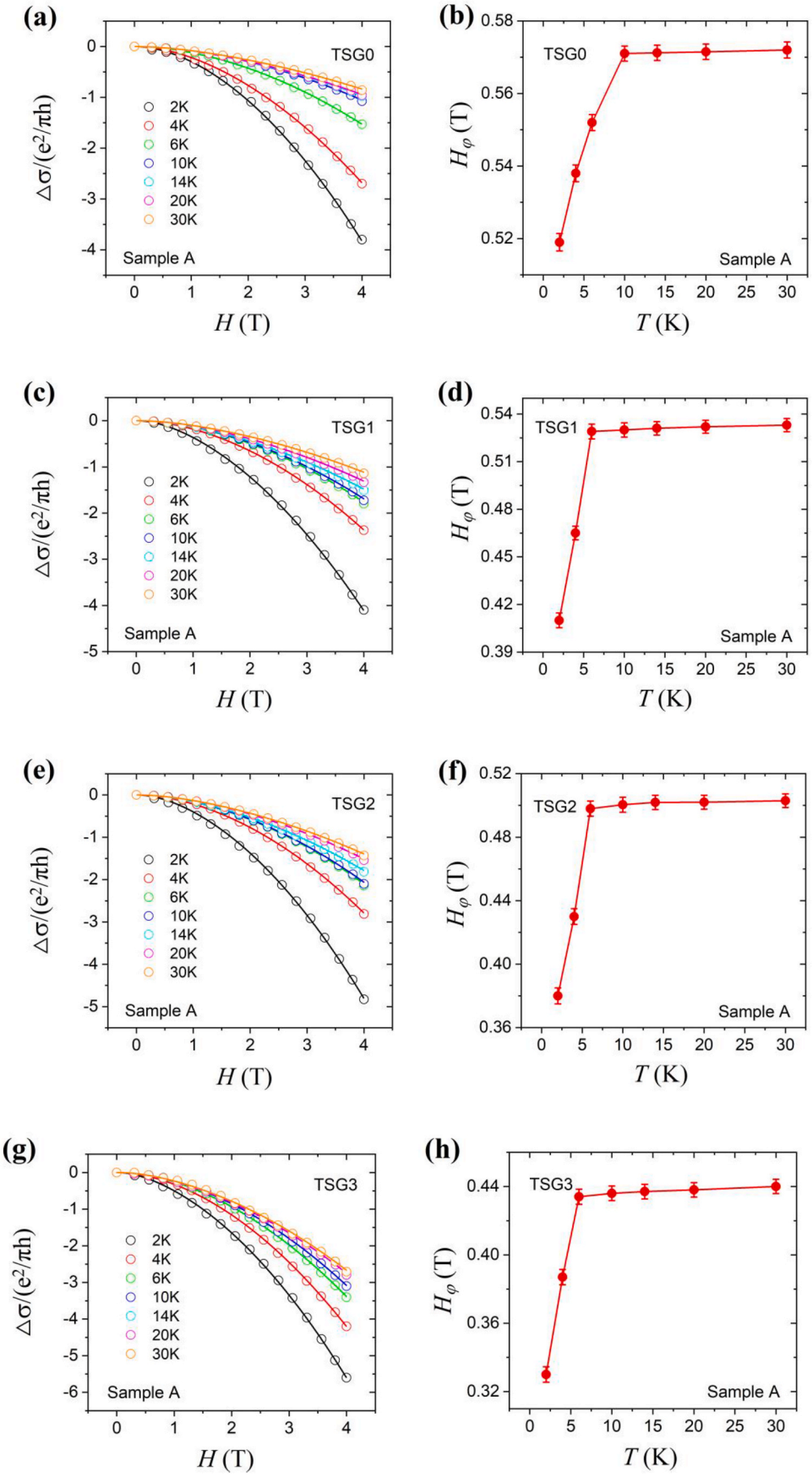

Fig. 3. $\triangle\sigma/\sigma_0$ as a function of magnetic field ($H\perp$interface) of sample A ((a), (c), (e), and (g)) under different TSGs from 2 K to 30 K, respectively. The solid curves are the best fitting to the HLN Eq. (4) by adding a H^2 term. The dependences between H_φ and T of sample A ((b), (d), (f), and (h)) under different TSGs.

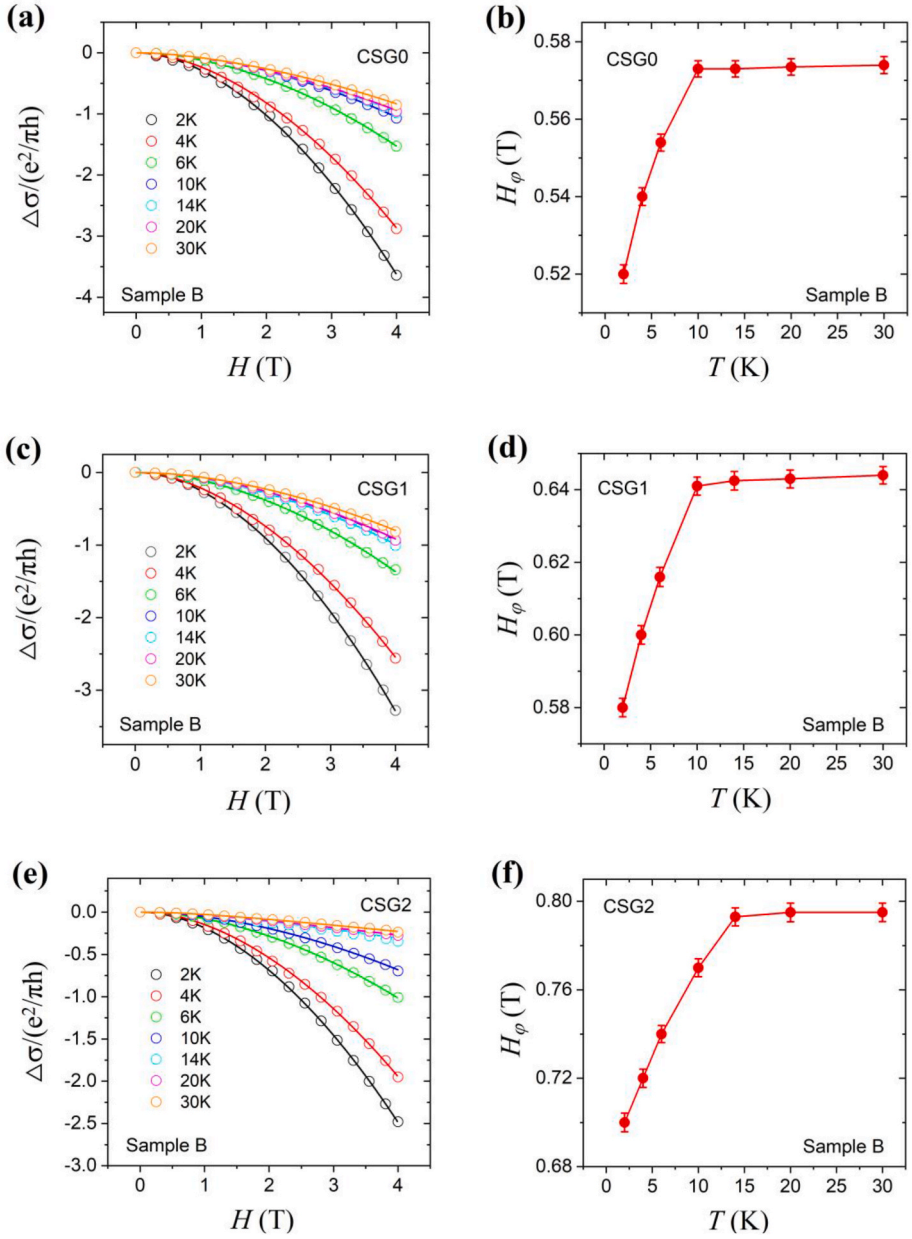

Fig. 4. $\triangle\sigma/\sigma_0$ as a function of magnetic field ($H\perp$interface) of sample B ((a), (c), and (e)) under different CSGs from 2 K to 30 K, respectively. The solid curves are the best fitting to the HLN Eq. (4) by adding a H^2 term. The dependences between H_φ and T of sample B ((b), (d), and (f)) under different CSGs.

deposition (PLD) at 790 °C in an oxygen pressure of 3×10^{-5} Torr. The repetition rate of laser pulse was 1 Hz and the fluence was 0.8 J/cm^2 (KrF, $\lambda = 248$ nm). After deposition, the samples were cooled down to room temperature without changing the oxygen pressure. The target-substrate distance was fixed at 5.6 cm.

The prepared samples were processed into a Hall bar using a standard ultraviolet lithography and wet etching technique (37% H_3PO_4 solution). To eliminate errors caused by the asymmetry of the Hall bar, all transport measurements were conducted under magnetic field reversal [25]. The transport properties were measured by Physical Property Measurement System (PPMS, Quantum Design) from 2 K to 300 K.

Two kinds of three-point mechanical bending apparatuses were designed to apply the tensile strain gradient (TSG) and compressive strain gradient (CSG). Both TSG and CSG are applied along [001] axis of the STO substrate. In particular, the same experimental results are obtained by applying TSG and CSG along [010] direction. All the bending apparatuses are made of brass, and strain gradients are applied by screws and spring pins (schematic structures, see the inset in Fig. 1(a) and (c)). In order to calculate the value of strain gradient, we put the samples with different strain gradients under a microscope and took photos at room temperature. W was estimated by drawing two horizontal lines in the photos. The range of w is almost 0.03–0.07 mm, and the effective length L_0 is almost 8–10 mm. As shown in Table 1, the magnitude of the strain gradients at the center of the samples with variant bending status are recorded. TSG is noted as positive and CSG is noted as negative [26]. According to the elastic theory, different strain gradients are calculated by Eq. (1) [27]:

$$\frac{\partial \varepsilon_{11}}{\partial x_3} = 3w\left(\frac{L_0}{2}\right)^{-2} \quad (1)$$

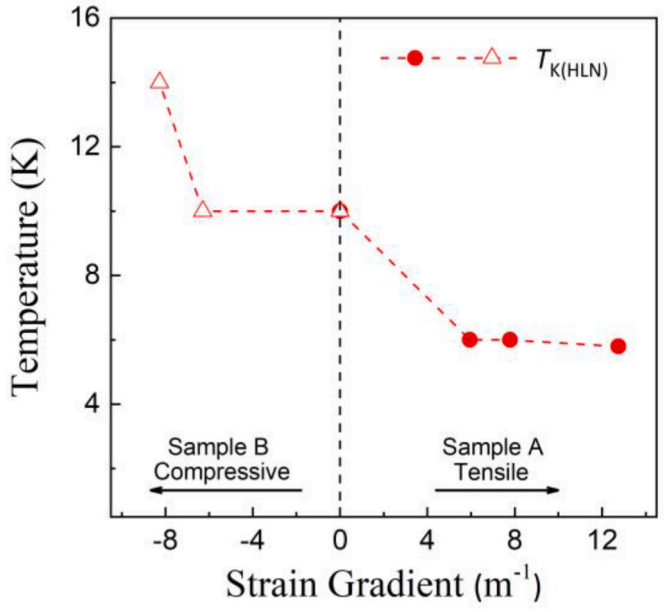

Fig. 5. The relationship between $T_{K(HLN)}$ and uniaxial strain gradients. The solid circles and hollow triangles represent $T_{K(HLN)}$ values under uniaxial tensile strain gradient (sample A) and uniaxial compressive strain gradient (sample B), respectively.

3. Results and discussion

3.1. Temperature dependences of resistance

To avoid any changes in the internal properties of the LAO/STO heterointerface after strain modulation, we fabricated two LAO/STO samples at identical deposition conditions for tensile (sample A) and compressive (sample B) experiments, respectively. Fig. 1 shows the temperature dependences of the sheet resistance (R_s) of the samples with TSGs and CSGs from 2 K to 300 K and the corresponding zoom-in on the low-temperature regions. It can be seen clearly that R_s begins to decrease when the temperature drops down. Meanwhile, it has a significant change on low-temperature regions. R_s decreases with TSG and increases with CSG. However, the resistance changes little at high temperature no matter what the sample is under TSG or CSG. Actually, a sharp increase of resistance of LAO/STO at higher temperatures is obvious, which could be attributed to complex coupling of the lattice, charge, and phonon [28]. The strain gradients have a slight effect on the resistance at high temperatures, much weaker than that on the low-temperature region and the relative change of R_s is very small, (here the relative change of R is defined as $(R_{strain} - R_0)/R_0$, R_{strain} and R_0 represent the resistance with and without the strain gradient, respectively), *i.e.* strain gradient has more significant impact on the relative change of R_s on the low-temperature region, especially below 20 K. In addition, owing to the fragility of the single crystal, the strain gradient could achieve a certain maximum. According to the measured value, the maximum TSG and CSG are +12.24 m^{-1} and -8.54 m^{-1}, respectively (Table 1). Otherwise, the samples are easily broken.

Notably, the sheet resistance R_s of the samples can be well modulated by the strain gradients and the R_s saturation behavior appears an upturn at low temperatures. The R_s -T curves around T_{min}, at which the resistance has a minimum, can be well described by Kondo model [29,30].

$$R_s(T) = R_0 + aT^2 + bT^5 + R_K\left(\frac{T}{T_{K(Kondo\ model)}}\right) \quad (2)$$

where R_0 is the residual resistance caused by sample disorder and the T^2 and T^5 terms are the contributions of electron-electron and phonon-electron interactions, respectively. An empirical form is used for the last term [31].

$$R_K\left(\frac{T}{T_{K(Kondo\ model)}}\right) = R_{K,0K}\left(\frac{T'^2_{K(Kondo\ model)}}{T^2 + T'^2_{K(Kondo\ model)}}\right)^S \quad (3)$$

where $T'_K = T_K/(2^{1/s}\text{-}1)^{1/2}$, $T_{K(Kondo\ model)}$ is the Kondo temperature, and s = 0.225 based on the result of the numerical renormalization-group (NRG) theory [31,32]. All the R_s-T curves were well fitted by Eq. (2) and Eq. (3) for different strain gradients. The fitted values of $T_{K(Kondo\ model)}$ are shown in Fig. 4.

It is clearly seen that the R_s saturation behavior appears an upturn at different strain gradients on low-temperature region. Kondo effect exists at the LAO/STO interface, which attributes to antiparallel spin scattering between localized magnetic moments and itinerant electrons, and always causes a minimum resistance. When the temperature decreases further, the localized magnetic scattering center is screened by the ambient antiparallel spins of itinerant electrons at the LAO/STO interface, thus Kondo scattering becomes weakened and R_s saturates gradually [33–35]. As shown in Fig. 1(b) and (d), the R_s-T curves in the low temperature area overlaps perfectly with the fitting curve according to the Kondo model, and the specific fitting parameters are shown in Tables 2 and 3. Fig. 2 shows the relationship between $T_{K(Kondo\ model)}$ and T_{min} and different uniaxial strain gradients.

3.2. Low field magneto-conductance

In order to study the effect of strain gradient on magnetoresistance,

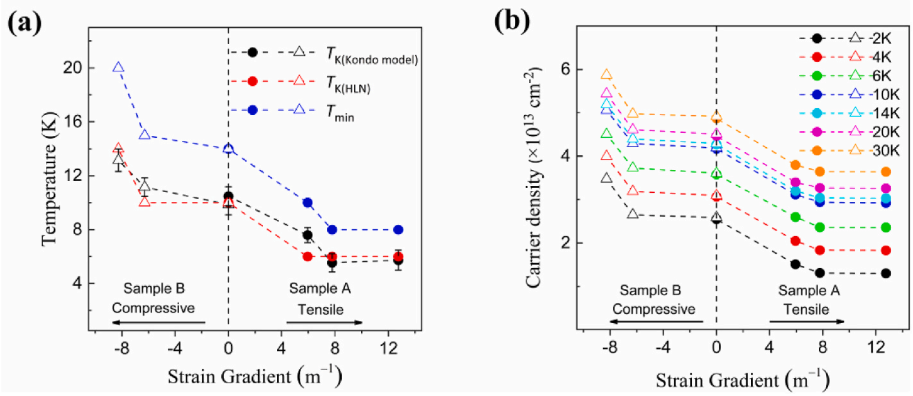

Fig. 6. (a) The relationship between $T_{K(Kondo\ model)}$, $T_{K(HLN)}$, T_{min} and the strain gradient. The sold circles and hollow triangles represent the data for sample An under TSG and for sample B under CSG, respectively. (b) Carrier density of sample A (solid circles) and sample B (hollow triangles), determined by the Hall coefficient acquired in a field of 9 T, under different strain gradients.

we utilize the low field magneto-conductance of 2DEG at the LAO/STO interface to analyze the temperature dependence of electron dephasing, based on the modified Hikami-Larkin-Nagaoka (HLN) equation [36,37]:

$$\triangle\sigma(H)=\sigma_{xx}(H)-\sigma_{xx}(H=0)=-\frac{\alpha e^2}{\pi h}\left[\ln\left(\frac{H_\varphi}{H}\right)-\psi\left(\frac{1}{2}+\frac{H_\varphi}{H}\right)\right] \quad (4)$$

σ_{xx} is defined by $\sigma_{xx}(H)=\left(\frac{R_{xx}(H)}{R_{xx}^2(H)+R_{xy}^2(H)}\right)$, where σ_{xx} is the magneto-conductance at a magnetic field, R_{xx} is the longitudinal magnetoresistance and R_{xy} is the Hall resistance, respectively. $\triangle\sigma$ (H) represents the change of magneto-conductance, ψ is the digamma function, e is the electronic charge, h is Planck's constant, $H_\varphi = h/8e\pi D\tau_\varphi$ is the characteristic magnetic field, D is the electronic diffusion constant, τ_φ is the phase coherence time and α is an effective constant that depends on the relative strengths of magnetic scattering and spin-orbital coupling. As shown in Figs. 3 and 4, different temperature dependences of the dephasing field H_φ are observed from 2 K to 30 K, which is consistent with the universal dephasing rate (proportional to H_φ) due to diluted Kondo impurities [38]. The dephasing field H_φ exhibits two distinct temperature dependences in different temperature ranges. Actually, it is another definition of $T_{K(HLN)}$ [39,40]. All the obtained values $T_{K(HLN)}$, at which the temperature dependence changes, are well consistent with that determined by the resistance measurements. Fig. 5 shows the relationship between $T_{K(HLN)}$ and different uniaxial strain gradients.

Fig. 6(a) shows the relationship between T_{min}, $T_{K(Kondo\ model)}$, $T_{K(HLN)}$ and the strain gradient. It can be clearly seen that $T_{K(Kondo\ model)}$ and $T_{K(HLN)}$ are well modulated by strain gradient. $T_{K(Kondo\ model)}$ and $T_{K(HLN)}$ increase with the compressive strain gradient. With the increase of CSG, $T_{K(Kondo\ model)}$ increases from 9.86 K to 13.12 K, and $T_{K(HLN)}$ increases from 10 K to 14 K. Conversely, they all decrease with the tensile strain gradient. With the increase of TSG, $T_{K(Kondo\ model)}$ decreases from 10.47 K to 5.73 K, and $T_{K(HLN)}$ decreases from 10 K to 6 K. T_{min} always shows the same strain gradient dependence as T_K, *i.e*, T_{min} decreases with the strain gradient from $-8.54\ m^{-1}$ to $+12.24\ m^{-1}$.

The decrease of T_K may be attributed to the change of carrier density [23] and/or to the modification of electronic band structure at the Fermi level [24] by the introduction of uniaxial strain gradient. Li et al. [41] reported the Kondo effect of electric field modulation in Gd:ZnO films and pointed out that carrier density n_s has an important modulation effect on T_K. They suggested that there was a specific relationship between T_K and the density of the electron state $D(E_F)$ near the Fermi level:

$$k_B T_K \sim e^{-1/|JD(E_F)|} \quad (5)$$

where k_B is Boltzmann constant, E_F is Fermi energy, and $J > 0$ is the antiferromagnetic coupling constant between the local magnetic moment and the traveling electron. Han et al. [42] also reported that T_K and carrier density in Nb:TiO_2 thin films showed the same variation trend. The carrier density n_s is the energy integral of $D(E)f(E)$, namely, $n = \int D(E)f(E)dE$, where $f(E)$ is the probability of electron occupation. Furthermore, according to the Schrieffer-Wolff formula [43], the Kondo coupling strength is

$$|JD|=\frac{\triangle}{\pi}\left[\frac{1}{|U+\varepsilon_d|}+\frac{1}{|\varepsilon_d|}\right] \quad (6)$$

where D is the density of state of the d_{xy} band, and JD is the Kondo coupling strength. U is the on-site Coulomb repulsion energy (U ≈ 2 eV in the LAO/STO interface 2DEG [44]). ε_d is the energy of the local d-level with respect to the Fermi energy E_F. $\triangle$ is the bandwidth of the local energy level, which is related to the hybrid intensity. In addition, in a strongly correlated electron system, according to the tightly bound approximation of the band theory, when the lattice constant shrinks, the bandwidth increases as the overlap of the wave functions of adjacent atoms increases. When LAO/STO is subjected to uniaxial compressive strain gradient, compared with LAO/STO in unstrained state, the lattice constant shrinks slightly, the overlap of adjacent atomic wave functions increases, and its bandwidth $\triangle$ increases accordingly. According to Eq. (6), when the Coulomb repulsion energy U, the energy ε_d of the local d level compared with the Fermi energy and the antiferromagnetic coupling constant J are constant, the larger the uniaxial compressive strain gradient, the larger the bandwidth $\triangle$, which leads to the larger density of state D. Based on Eq. (5), the higher the density of state D, the higher the Kondo temperature T_K. On the contrary, the lattice constant of LAO/STO under uniaxial tensile state slightly expands compared with that without strain, resulting in a decrease in bandwidth $\triangle$ and a decrease in band electronic state density D, ultimately reducing T_K.

Zhang et al. [24]. Also used density functional theory to calculate the density of state of d_{xy} band of 3d Ti atoms in LAO/STO system under different uniaxial strain states, and confirmed that the density of state of d_{xy} band in the compressive state was the highest, while the density of state of d_{xy} band in the tensile state was the lowest. They also estimated the different carrier densities of LAO/STO under different strain states by applying 3% tensile strain and 3% compressive strain respectively, and obtained carrier densities of $2.2 \times 10^{13}\ cm^{-2}$ and $3.14 \times 10^{13}\ cm^{-2}$ under tensile and compressive strain states, respectively. It is shown that strain can effectively modulate the density of state and carrier density in the LAO/STO system.

Fig. 6(b) shows the relationship between the carrier density and the strain gradient from 2 K to 30 K for sample A and sample B, in which the carrier density was determined by the Hall coefficient in a field of 9 T. Notably, the carrier density at various temperatures shows the same decrease trend as T_K with the strain gradient ranging from $-8.54\ m^{-1}$ to $+12.24\ m^{-1}$. Anyhow, it should be emphasized that the phenomena of strain-gradient-modulated Kondo effect at the LAO/STO interface are doubly confirmed by the fittings based on the formula of Kondo model and HLN equation, respectively. It is worth noting that the Kondo effect is an archetype for the emergent magnetic interactions amongst localized and delocalized electrons at the LAO/STO heterointerface [45,46], and it may be attributed to the intrinsic localized magnetic Ti^{3+} ions by many studies [45,47–49]. More importantly, the ability to produce and modulate the effect by purely external means in any conducting system is of interest in its own right.

4. Conclusions

In conclusion, we demonstrated that Kondo effect at the LAO/STO interface is well modulated by the strain gradients, which is related to the carrier density. T_K and T_{min} decrease with the increase of tensile strain gradient. On the contrary, T_K and T_{min} increase with compressive strain gradient. These results not only promote the understanding of complex oxide interfaces, but also provide new possibilities for the application design in practical electronic devices. For example, the strain-gradient-modulated Kondo scattering may be further adopted to regulate applications of the Kondo effect, such as the spin Hall effect [50] and thermoelectricity [51].

Declaration of competing interest

The authors declare that they have no known competing financial interests or personal relationships that could have appeared to influence the work reported in this paper.

Data availability

No data was used for the research described in the article.

Acknowledgements

We thank the National Natural Science Foundation of China (Grants Nos. 92065110, 11974048, and 12074334) for their financial support.

References

[1] A.C. Hewson, The Kondo Problem to Heavy Fermions, Cambridge University Press, 1997.

[2] V. Madhavan, W. Chen, T. Jamneala, M.F. Crommie, N.S. Wingreen, Tunneling into a single magnetic atom: spectroscopic evidence of the Kondo resonance, Science 280 (1998) 567–569.

[3] A. Zhao, Q. Li, L. Chen, H. Xiang, W. Wang, S. Pan, B. Wang, X. Xiao, J. Yang, J. G. Hou, Q. Zhu Controlling the Kondo effect of an adsorbed magnetic ion through its chemical bonding, Science 309 (2005) 1542–1544.

[4] A. Ohtomo, H.Y. Hwang, A high-mobility electron gas at the $LaAlO_3/SrTiO_3$ heterointerface, Nature 427 (2004) 423–426.

[5] Y.Z. Chen, F. Trier, T. Wijnands, R.J. Green, N. Gauquelin, R. Egoavil, D. V. Christensen, G. Koster, M. Huijben, N. Bovet, S. Macke, F. He, R. Sutarto, N. H. Andersen, J.A. Sulpizio, M. Honig, G.E.D.K. Prawiroatmodjo, T.S. Jespersen, S. Linderoth, S. Ilani, J. Verbeeck, G. Van Tendeloo, G. Rijnders, G.A. Sawatzky, N. Pryds, Extreme mobility enhancement of two-dimensional electron gases at oxide interfaces by charge-transfer-induced modulation doping, Nat. Mater. 14 (2015) 801–806.

[6] H. Liang, L. Cheng, L. Wei, Z. Luo, G. Yu, C. Zeng, Z. Zhang, Nonmonotonically tunable Rashba spin-orbit coupling by multiple-band filling control in SrTiO3-based interfacial d-electron gases, Phys. Rev. B 92 (2015), 075309.

[7] E. Lesne, Yu Fu, S. Oyarzun, J.C. Rojas-Sánchez, D.C. Vaz, H. Naganuma, G. Sicoli, J.-P. Attané, M. Jamet, E. Jacquet, J.-M. George, A. Barthélémy, H. Jaffrès, A. Fert, M. Bibes, L. Vila, Highly efficient and tunable spin-to-charge conversion through Rashba coupling at oxide interfaces, Nat. Mater. 15 (2016) 1261–1266.

[8] S. Hurand, A. Jouan, C. Feuillet-Palma, G. Singh, J. Biscaras, E. Lesne, N. Reyren, A. Barthélémy, M. Bibes, J.E. Villegas, C. Ulysse, X. Lafosse, M. Pannetier-Lecoeur, S. Caprara, M. Grilli, J. Lesueur, N. Bergeal, Field-effect control of superconductivity and Rashba spin-orbit coupling in top-gated $LaAlO_3/SrTiO_3$ devices, Sci. Rep. 5 (2015), 12751.

[9] L. Li, C. Richter, J. Mannhart, R.C. Ashoori, Coexistence of magnetic order and two-dimensional superconductivity at $LaAlO_3/SrTiO_3$ interfaces, Nat. Phys. 7 (2011) 762–766.

[10] J.A. Bert, B. Kalisky, C. Bell, M. Kim, Y. Hikita, H.Y. Hwang, K.A. Moler, Direct imaging of the coexistence of ferromagnetism and superconductivity at the $LaAlO_3/SrTiO_3$ interface, Nat. Phys. 7 (2011) 767.

[11] K. Han, N. Palina, S.W. Zeng, Z. Huang, C.J. Li, W.X. Zhou, D.Y. Wan, L.C. Zhang, X. Chi, R. Guo, J.S. Chen, T. Venkatesan, A. Rusydi, Ariando, controlling kondo-like scattering at the $SrTiO_3$-based interfaces, Sci. Rep. 6 (2016), 25455.

[12] A. Brinkman, M. Huijben, M.van. Zalk, J. Huijben, U. Zeitler, J.C. Maan, W.G. van der Wiel, G. Rijnders, D.H.A. Blank, H. Hilgenkamp, Magnetic effects at the interface between non-magnetic oxides, Nat. Mater. 6 (2007) 493–496.

[13] H. Xue, Y. Hong, C. Li, J. Meng, Y. Li, K. Liu, M. Liu, W. Jiang, Z. Zhang, L. He, R. Dou, C. Xiong, J. Nie, Large negative magnetoresistance driven by enhanced weak localization and Kondo effect at the interface of LaAlO3 and Fe-doped SrTiO3, Phys. Rev. B 98 (2018), 085305.

[14] A.D. Caviglia, S. Gariglio, N. Reyren, D. Jaccard, T. Schneider, M. Gabay, S. Thiel, G. Hammerl, J. Mannhart, J.- M Triscone, Electric field control of the $LaAlO_3/SrTiO_3$ interface ground state, Nature 456 (2008) 624–627.

[15] A. Tebano, E. Fabbri, D. Pergolesi, G. Balestrino, E. Traversa, Room-temperature giant persistent photoconductivity in SrTiO3/LaAlO3 heterostructures, ACS Nano 6 (2012) 1278–1283.

[16] Y. Xie, Y. Hikita, C. Bell, H.Y. Hwang, Control of electronic conduction at an oxide heterointerface using surface polar adsorbates, Nat. Commun. 2 (2011) 494.

[17] S. Nazir, K. Yang, First-Principles Characterization of the critical thickness for forming metallic states in strained LaAlO3/SrTiO3(001) heterostructure, ACS Appl. Mater. Interfaces 6 (2014) 22351–22358.

[18] S. Nazir, M. Behtash, K. Yang, Enhancing interfacial conductivity and spatial charge confinement of $LaAlO_3/SrTiO_3$ heterostructures via strain engineering, Appl. Phys. Lett. 105 (2014), 141602.

[19] C.W. Bark, D.A. Felker, Y. Wang, Y. Zhang, H.W. Jang, C.M. Folkman, J.W. Park, S. H. Baek, H. Zhou, D.D. Fong, X.Q. Pan, E.Y. Tsymbal, M.S. Rzchowski, C.B. Eom, Tailoring a two-dimensional electron gas at the LaAlO3/SrTiO3 (001) interface by epitaxial strain, P. Natl. Acad. Sci. 108 (2011) 4720–4724.

[20] Z. Huang, Z.Q. Liu, M. Yang, S.W. Zeng, A. Annadi, W.M. Lü, X.L. Tan, P.F. Chen, L. Sun, X. Renshaw Wang, Y.L. Zhao, C.J. Li, J. Zhou, K. Han, W.B. Wu, Y.P. Feng, J.M.D. Coey, T. Venkatesan, Ariando, Biaxial strain-induced transport property changes in atomically tailored $SrTiO_3$-based systems, Phys. Rev. B 90 (2014), 125156.

[21] Y. Du, C. Wang, J. Li, X. Zhang, F. Wang, Y. Zhu, N. Yin, L. Mei, The effect of in-plane strain on the electronic properties of LaAlO3/SrTiO3 interface, Comput. Mater. Sci. 99 (2015) 57–61.

[22] Q. Gan, R.A. Rao, C.B. Eom, Direct measurement of strain effects on magnetic and electrical properties of epitaxial $SrRuO_3$ thin films, Appl. Phys. Lett. 72 (1998) 978.

[23] Z. Zhang, W. Jiang, K. Liu, M. Liu, J. Meng, L. Wu, T. Shao, J. Ling, C. Yao, C. Xiong, R. Dou, J. Nie, Strain-gradient-induced modulation of carrier density and mobility at the $LaAlO_3/SrTiO_3$ heterointerface, Ann. Phys. 532 (2020), 2000155.

[24] F. Zhang, Y. Fang, N.Y. Chan, W.C. Lo, D.F. Li, C. Duan, F. Ding, J.Y. Dai, Dynamic modulation of the transport properties of the LaAlO3/SrTiO3 interface using uniaxial strain, Phys. Rev. B 93 (2016), 214427.

[25] H. Xue, C. Li, Y. Hong, X. Wang, Y. Li, K. Liu, W. Jiang, M. Liu, L. He, R. Dou, C. Xiong, J. Nie, Temperature dependence of the conductive layer thickness at the LaAlO3/SrTiO3 heterointerface, Phys. Rev. B 96 (2017), 235310.

[26] F. Zhang, P. Lv, Y. Zhang, S. Huang, C.M. Wong, H. M Yau, X. Chen, Z. Wen, X. Jiang, C. Zeng, J. Hong, J. Dai, Modulating the electrical transport in the two-dimensional electron gas at LaAlO3/SrTiO3 heterostructures by interfacial flexoelectricity, Phys. Rev. Lett. 122 (2019), 257601.

[27] P. Zubko, G. Catalan, A. Buckley, P.R.L. Welche, J.F. Scott, Strain-gradient-induced polarization in SrTiO3 single crystals, Phys. Rev. Lett. 99 (2007), 167601.

[28] C. Cancellieri, A.S. Mishchenko, U. Aschauer, A. Filippetti, C. Faber, O.S. Barišić, V. A. Rogalev, T. Schmitt, N. Nagaosa, V.N. Strocov, Polaronic metal state at the $LaAlO_3/SrTiO_3$ interface, Nat. Commun. 7 (2016) 1–8.

[29] M. Lee, J.R. Williams, S. Zhang, C.D. Frisbie, D.G. Gordon, Electrolyte gate-controlled Kondo effect in SrTiO3, Phys. Rev. Lett. 107 (2011), 256601.

[30] J.Y. Yang, Y.L. Han, L. He, R.F. Dou, C.M. Xiong, J.C. Nie, *d* carrier induced intrinsic room temperature ferromagnetism in Nb:TiO_2 film, Appl. Phys. Lett. 100 (2012), 202409.

[31] D. Goldhaber-Gordon, J. Gores, M.A. Kastner, H. Shtrikman, D. Mahalu, U. Meirav, From the Kondo regime to the mixed-valence regime in a single-electron transistor, Phys. Rev. Lett. 81 (1998) 5225.

[32] T.A. Costi, A.C. Hewson, V. Zlatic, Transport coefficients of the Anderson model via the numerical renormalization group, J. Phys. Condens. Matter 6 (1994) 2519.

[33] S. Das, A. Rastogi, L. Wu, J.C. Zheng, Z. Hossain, Y. Zhu, R.C. Budhani, Kondo scattering in δ-doped LaTiO3/SrTiO3 interfaces: renormalization by spin-orbit interactions, Phys. Rev. B 90 (2014), 081107.

[34] S. Zhang, S.B. Ogale, W. Yu, X. Gao, T. Liu, S. Ghosh, G.P. Das, A.T.S. Wee, R. L. Greene, T. Venkatesan, Electronic manifestation of cation-vacancy-induced magnetic moments in a transparent oxide semiconductor: anatase Nb:TiO_2, Adv. Mater. 21 (2009) 2282–2287.

[35] J. Kondo, Resistance minimum in dilute magnetic alloys, Prog. Theor. Phys. 32 (1964) 37–49.

[36] S. Hikami, A.I. Larkin, Y. Nagaoka, Spin-orbit interaction and magnetoresistance in the two dimensional random system, Prog. Theor. Phys. 63 (1980) 707–710.

[37] R. Sultana, G. Gurjar, P. Neha, S. Patnaik, V.P.S. Awana, Hikami-Larkin-Nagaoka (HLN) treatment of the magneto-conductivity of Bi_2Te_3 topological insulator, J. Supercond. Nov. Magn. 31 (2018) 2287–2290.

[38] T. Micklitz, A. Altland, T.A. Costi, A. Rosch, Universal dephasing rate due to diluted Kondo impurities, Phys. Rev. Lett. 96 (2006), 226601.

[39] R.P. Peters, G. Bergmann, R.M. Mueller, Kondo maximum of magnetic scattering, Phys. Rev. Lett. 58 (1987) 1964–1967.

[40] C. Van Haesendonck, J. Vranken, Y. Bruynseraede, Resonant Kondo scattering of weakly localized electrons, Phys. Rev. Lett. 58 (1987) 1968–1971.

[41] Y. Li, R. Deng, W. Lin, Y. Tian, H. Peng, J. Yi, B. Yao, T. Wu, Electrostatic tuning of Kondo effect in a rare-earth-doped wide-band-gap oxide, Phys. Rev. B 87 (2013), 155151.

[42] Y.L. Han, Z.Z. Luo, C.J. Li, S.C. Shen, G.L. Qu, C.M. Xiong, R.F. Dou, L. H, J.C. Nie, Carrier-mediated Kondo effect and Hall mobility by electrolyte gating in slightly doped anatase TiO2 films, Phys. Rev. B 90 (2014), 205107.

[43] A.C. Hewson, The Kondo Problem to Heavy Fermions, Cambridge University Press, London, 1997.

[44] J.M. Edge, Y. Kedem, U. Aschauer, S.A. Nicola, V.B. Alexander, Quantum critical origin of superconducting dome in SrTiO3, Phys. Rev. Lett. 115 (2015), 247002.

[45] K.X. Jin, W. Lin, B.C. Luo, T. Wu, Photoinduced modulation and relaxation characteristics in LaAlO3/SrTiO3 heterointerface, Sci. Rep. 5 (2015) 8778.

[46] W. Lin, J. Ding, S. Wu, S. Wu, Y. Li, J. Lourembam, S. Shannigrahi, S.J. Wang, T. Wu, Electrostatic modulation of $LaAlO_3/SrTiO_3$ interface transport in an electric double-layer transistor, Adv. Mater. Interfac. 1 (2014), 1300001.

[47] R. Pentcheva, W.E. Pickett, Charge localization or itineracy at LaAlO3/SrTiO3 interfaces: hole polarons, oxygen vacancies, and mobile electrons, Phys. Rev. B 74 (2006), 035112.

[48] J.-S. Lee, Y.W. Xie, H.K. Sato, C. Bell, Y. Hikita, H.Y. Hwang, C.C. Kao, Titanium d_{xy} ferromagnetism at the $LaAlO_3/SrTiO_3$ interface, Nat. Mater. 12 (2013) 703–706.

[49] S. Banerjee, O. Erten, M. Randeria, Ferromagnetic exchange, spin–orbit coupling and spiral magnetism at the $LaAlO_3/SrTiO_3$ interface, Nat. Phys. 9 (2013) 626–630.

[50] G.Y. Guo, S. Maekawa, N. Nagaosa, Enhanced spin Hall effect by resonant skew scattering in the orbital-dependent Kondo effect, Phys. Rev. Lett. 102 (2009), 036401.

[51] J. Wu, Y. Liu, Y. Liu, Y. Cai, Y. Zhao, H.K. Ng, K. Watanabe, T. Taniguchi, G. Zhang, C. Qiu, D. Chi, A.H. Castro Neto, J.T.L. Thong, K.P. Loh, K. Hippalgaonkar, Kondo impurities in two dimensional MoS_2 for achieving ultrahigh thermoelectric powerfactor, arXiv 1901 (2019), 04661.